

2008

Influence of phonon scattering on the performance of p-i-np-i-n band-to-band tunneling transistors

Siyuranga O. Koswatta
Purdue University, koswatta@purdue.edu

Mark S. Lundstrom
Purdue University, lundstro@purdue.edu

Dmitri E. Nikonov
Intel Corporation, Components Research

Follow this and additional works at: <https://docs.lib.purdue.edu/ecepubs>

 Part of the [Electrical and Computer Engineering Commons](#)

Koswatta, Siyuranga O.; Lundstrom, Mark S.; and Nikonov, Dmitri E., "Influence of phonon scattering on the performance of p-i-np-i-n band-to-band tunneling transistors" (2008). *Department of Electrical and Computer Engineering Faculty Publications*. Paper 131.
<http://dx.doi.org/10.1063/1.2839375>

This document has been made available through Purdue e-Pubs, a service of the Purdue University Libraries. Please contact epubs@purdue.edu for additional information.

Influence of phonon scattering on the performance of *p-i-n* band-to-band tunneling transistors

Siyuranga O. Koswatta^{a)} and Mark S. Lundstrom

School of Electrical and Computer Engineering, Purdue University, West Lafayette, Indiana 47907-1285, USA

Dmitri E. Nikonov

Technology and Manufacturing Group, Intel Corp., SC1-05, Santa Clara, California 95052, USA

(Received 11 October 2007; accepted 11 January 2008; published online 31 January 2008)

Power dissipation has become a major obstacle in performance scaling of modern integrated circuits and has spurred the search for devices operating at lower voltage swing. In this letter, we study *p-i-n* band-to-band tunneling field effect transistors taking semiconducting carbon nanotubes as the channel material. The on current of these devices is mainly limited by the tunneling barrier properties, and phonon-scattering has only a moderate effect. We show, however, that the off current is limited by phonon absorption assisted tunneling, and thus is strongly temperature dependent. Subthreshold swings below the 60 mV/decade conventional limit can be readily achieved even at room temperature. Interestingly, although subthreshold swing degrades due to the effects of phonon scattering, it remains low under practical biasing conditions. © 2008 American Institute of Physics. [DOI: 10.1063/1.2839375]

As integrated circuit densities continue to increase, power dissipation has become a critical issue. Silicon metal-oxide-semiconductor field-effect transistors (MOSFETs) now operate with a power supply voltage of approximately 1 V.¹ A key challenge for device research is to develop high performance transistors that operate at substantially lower voltages. To maintain high on currents at lower voltages, it is likely that devices will need to operate with the subthreshold swing below the conventional MOSFET limit of 60 mV/decade (at room temperature). Band-to-band tunneling (BTBT) transport in devices has been proposed²⁻⁷ and demonstrated⁸⁻¹³ as one means to produce low-voltage transistors. The BTBT FET device concept is currently being explored in many material systems including those based on carbon nanotubes¹⁴⁻¹⁹ (CNTs) and silicon.²⁰ CNTs are especially promising for such devices because their small effective masses and direct bandgap²¹ promote BTBT. Furthermore, physically detailed simulation techniques have been developed^{22,23} and thoroughly benchmarked against experimental results,²⁴⁻²⁶ so a tool to explore device design and optimization is available.

Our objective in this letter is to identify the physical mechanisms that limit the performance of a BTBT FET, specifically the maximum on-state current, off-state current, and the steepness of the on-off transition. We use the carbon nanotube BTBT FET as a model device to address these questions because of the aforementioned benefits of this system. Our earlier work has shown that BTBT in a CNT-MOSFET-type structure is dominated by phonon assisted inelastic tunneling that leads to degradation of desirable device characteristics.^{25,27} Here, we examine another popular tunneling device structure based on gated *p-i-n* geometry (*p-i-n* TFET).^{2-5,7,15,16} The purpose of this letter is to examine how phonon scattering affects the performance of such devices. Although we use the CNT as a model device, the general conclusions are expected to be broadly applicable to this

class of devices fabricated in different materials.

The model device structure used in this study, shown in Fig. 1, has a cylindrical wrap-around gate and doped source/drain regions (see caption for device parameters). We have performed dissipative quantum transport calculations using the nonequilibrium Green's function formalism²⁸ along with self-consistent electrostatics. A detailed description of the simulation procedure is presented in Ref. 23. The device Green's function G at an energy E in the presence of electron-phonon (e-ph) scattering is given by²⁸ $G = [EI - H_{pz} - \Sigma_{S/D} - \Sigma_{scat}]^{-1}$, where I is the identity matrix and H_{pz} is the device Hamiltonian in the nearest-neighbor tight-binding description.²¹ Here, the mode-space treatment for carrier transport is used.^{23,29} We are considering the lowest conduction band and the highest valence band with twofold spin and twofold valley degeneracies.²¹ $\Sigma_{S/D}$ and Σ_{scat} are the self-energy functions (energy dependent) arising due to coupling to the semi-infinite source/drain contacts and due to electron-phonon interaction, respectively. The imaginary part of the scattering self-energy function, $\text{Im}(\Sigma_{scat})$, is related to the in/out-scattering functions $\Sigma_{scat}^{in/out}$ by $\text{Im}(\Sigma_{scat}) = -i(\Sigma_{scat}^{in} + \Sigma_{scat}^{out})/2$. The real part of Σ_{scat} is estimated to be a minor correction and is ignored in this work to minimize computational complexity.²³

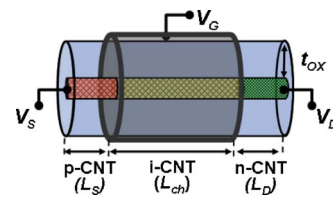


FIG. 1. (Color online) Modeled CNT *p-i-n* TFET structure with wrap-around gate used in this study. A (16,0) zigzag CNT with high- k HfO_2 ($k=16$, $t_{ox}=2$ nm) gate oxide, intrinsic channel ($L_{ch}=20$ nm), doped source (*p*-type, $N_S=0.75/\text{nm}$, $L_S=35$ nm) and drain (*n*-type, $N_D=0.75/\text{nm}$, $L_D=35$ nm) have been used. Source/drain doping levels can be compared to the carbon atom density in a (16,0) CNT of 150.2/nm.

^{a)}Electronic mail: koswatta@purdue.edu.

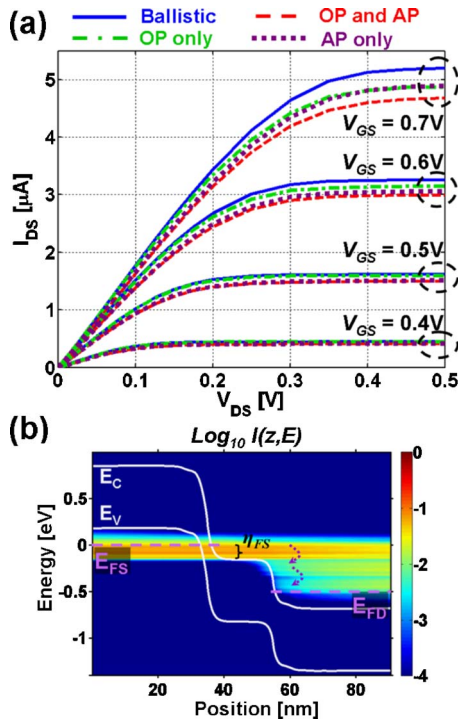


FIG. 2. (Color online) (a) Above-threshold $I_{DS}-V_{DS}$ characteristics for the CNT $p-i-n$ TFET in Fig. 1. All the optical phonon modes (LO, ZBO, and RBM) are considered simultaneously for OP scattering. LA mode is considered for AP scattering. (b) Energy-position resolved current density spectrum at $V_{DS}=V_{GS}=0.5$ V confirms the reduced influence of high-energy OP scattering on dc current transport up to moderate gate biases.

The in/out-scattering functions for an optical phonon (OP) mode with energy $\hbar\omega$ are given by²⁸

$$\begin{aligned} \Sigma_{\text{scat}}^{\text{in,out}}(E) = & D_0(n_\omega + 1)G^{n,p}(E \pm \hbar\omega) \\ & + D_0n_\omega G^{n,p}(E \mp \hbar\omega), \end{aligned} \quad (1)$$

where D_0 is the e-ph coupling parameter calculated according to Ref. 30, and $G^{n,p}$ are the electron/hole correlation functions given by²⁸ $G^{n,p} = G \Sigma^{\text{in,out}} G^\dagger$, where $\Sigma^{\text{in,out}}$ have contributions from both e-ph scattering [Eq. (1)] as well as coupling to the contact reservoirs. OP scattering by 190 meV longitudinal optical (LO) mode, 180 meV zone-boundary (ZBO) mode, and 21 meV radial-breathing mode (RBM) have been considered. Acoustic phonon (AP) scattering is by the longitudinal acoustic (LA) mode.²³ The phonon population is assumed to be in thermal equilibrium, with the number, n_ω , given by the Bose-Einstein distribution $n_\omega = [\exp(\hbar\omega/k_B T) - 1]^{-1}$, where k_B is the Boltzmann constant and T the device temperature. The first term in the right hand side of Eq. (1) corresponds to phonon emission mediated processes, while the second term corresponds to phonon absorption. Finally, the current through the device is calculated from Eq. (17) of Ref. 23.

The above-threshold (on-state) operation is discussed first. Figure 2(a) compares the output characteristics, $I_{DS}-V_{DS}$, of the CNT $p-i-n$ TFET under ballistic and dissipative transport. Here, it is seen that the influence of OP scattering (green dash-dot) becomes important only at large gate biases, even though the high-energy modes (LO and ZBO) have the strongest e-ph coupling.²³ Up to moderate gate biases, the current reduction is mainly due to carrier backscattering by AP and low-energy (RBM) phonon modes. Similar behavior on the influence of phonon scattering on the above-threshold

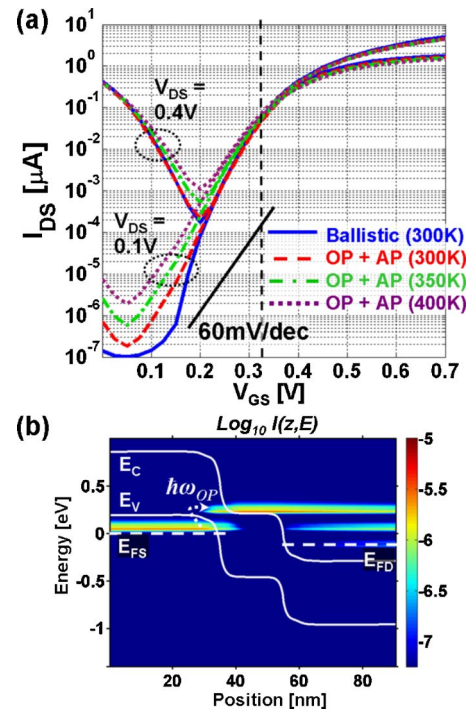


FIG. 3. (Color online) (a) $I_{DS}-V_{GS}$ characteristics for the CNT $p-i-n$ TFET in Fig. 1 at $V_{DS}=0.1$ V and 0.4 V with and without phonon scattering. Simulated device temperatures are as shown in the legend. It is observed that the presence of phonons degrades the subthreshold swing. (b) Energy-position resolved current density spectrum at a device temperature of 400 K ($V_{GS}=0.125$ V, $V_{DS}=0.1$ V). Phonon absorption assisted transport is clearly observed at the source-channel junction. Carriers thermalize after reaching the drain.

operation of CNT-MOSFETs has already been reported²³ and can be easily understood as follows. In order to have current reduction due to scattering by high-energy phonons, a majority of forward-going carriers (source \rightarrow drain) should be backscattered into empty backward-going states by OP emission. Thus, the energy requirements for effective backscattering depend on the condition $(E_{FS} - E_{C-\text{channel}}) = \eta_{FS} \geq \hbar\omega$, where E_{FS} and $E_{C-\text{channel}}$ are the source Fermi level and the channel conduction band position, respectively [see Fig. 2(b)].²³ This is further exemplified in the energy-position resolved current density spectrum shown in Fig. 2(b). After reaching the drain region, however, carriers can be efficiently scattered by OP emission down to empty low-lying states, and thus will not possess enough energy to surmount the channel barrier and reach the source region again. On the other hand, elastic scattering due to acoustic and low-energy phonons can effectively backscatter at all gate biases and is the dominant mechanism until high-energy OP scattering becomes effective at larger gate biases. Therefore, in CNT $p-i-n$ TFETs, above-threshold performance is only moderately affected by phonon scattering. We observe, however, a lower value of the on current (by about four to ten times) in the CNT $p-i-n$ TFET compared to that of conventional CNT-MOSFETs (Ref. 23) due to the presence of the tunneling barrier. This observation confirms that the on-state performance of $p-i-n$ TFETs is mainly dominated by the tunneling barrier properties and moderately affected by the channel itself.^{5,7,19}

The subthreshold (off-state) operation is discussed next. Figure 3(a) shows the transfer characteristics, $I_{DS}-V_{GS}$, for the CNT $p-i-n$ TFET. Note that all the phonon modes are

treated simultaneously under dissipative transport even though only the 180meV ZBO mode, with strongest e-ph coupling, is seen to mainly affect the subthreshold properties. In Fig. 3(a) it is seen that the *p-i-n* TFET has ambipolar behavior, which can be easily understood by observing Fig. 2(b). For small gate biases (or negative biases), the bands in the channel are pulled up and a tunneling path appears at the channel-drain junction leading to ambipolar transport. As expected, the ambipolar branch appears earlier for larger drain biases. For identical source/drain doping concentrations, the $I_{DS}-V_{GS}$ curves are symmetric around the minimum point. Asymmetric doping schemes can, however, suppress the ambipolar branch down to smaller gate biases and lead to more desirable device characteristics.¹⁶ It should be noted that, unlike in a conventional MOSFET, the subthreshold swing (S) of a *p-i-n* TFET is not a constant, but is bias dependent, as seen in Fig. 3(a).^{5,6,19} Interestingly, we observe less than 60 mV/decade S at room temperature ($T=300$ K) for both ballistic and dissipative transport (blue solid and red dashed curves); in our model device, $S < 60$ mV/decade is obtained for $V_{GS} < 0.32$ V (left of dashed vertical line).

In Fig. 3(a), it is evident that the presence of OPs has a significant detrimental effect on the subthreshold properties; a minimum S of 20 mV/decade for ballistic transport (at $V_{DS}=0.1$ V) degrades to 40 mV/decade in the presence of OPs at room temperature. The degradation is even greater at higher device temperatures; minimum $S \approx 50$ mV/decade at $T=400$ K ($V_{DS}=0.1$ V). The main reason for such deterioration of S is due to phonon absorption-assisted transport as exemplified in Fig. 3(b). Under the ballistic approximation, the minimum off-state current is mainly due to direct source to drain tunneling through the channel barrier region and can be made very small; longer channel lengths L_{ch} further suppresses the off current, and $S < 10$ mV/decade can be achieved for ballistic transport. From Eq. (1) it is seen that the phonon absorption assisted process is proportional to the phonon occupation number n_{ω} and increases at higher device temperatures. Thus, even though the direct tunneling processes are expected to be fairly temperature independent,^{5,6,19} higher-order processes such as phonon assisted transport that are temperature dependent can become important in the off state of a BTBT device, limiting the desirable characteristics that could have been achieved otherwise. The influence of two-phonon absorption of high-energy OPs, however, is expected to be insignificant due to negligible e-ph coupling that is proportional to $\sim n_{\omega}^2$.³¹ On the other hand, the on-state performance of the CNT *p-i-n* TFET is observed to be relatively temperature insensitive because the above-threshold transport is mainly due to direct tunneling. In indirect band-gap semiconductors, such as technologically important silicon and germanium, BTBT would be mainly due to phonon assisted transport,³² and could have strong temperature dependence both in the off state as well as the on state.

In conclusion, we observe less than 60 mV/decade subthreshold swings in *p-i-n* TFETs, in contrast to that in conventional (e.g., *n-i-n*) MOSFETs operating in the over-the-barrier conduction regime. The on-current of *p-i-n* TFETs is, however, mainly dependent on the tunneling barrier properties, and phonon scattering has only a moderate effect. On the other hand, the subthreshold operation is dominated by

phonon assisted transport, and exhibits significant temperature dependence. Nevertheless, the low subthreshold swing is robust and persists even with the inclusion of phonon scattering and under practical source-to-drain biasing conditions.

S.O.K. thanks the Intel Foundation for Ph.D. Fellowship support. Computational support was provided by the NSF Network for Computational Nanotechnology (NCN).

¹International Technology Roadmap for Semiconductors (ITRS) (www.itrs.net).

²S. Banerjee, W. Richardson, J. Coleman, and A. Chatterjee, IEEE Electron Device Lett. **ED-8**, 347 (1987).

³T. Baba, Jpn. J. Appl. Phys., Part 2 **31**, 455 (1992).

⁴W. Hansch, C. Fink, J. Schulze, and I. Eisele, Thin Solid Films **369**, 387 (2000).

⁵K. K. Bhuiwarka, J. Schulze, and I. Eisele, IEEE Trans. Electron Devices **52**, 909 (2005).

⁶Q. Zhang, W. Zhao, and A. Seabaugh, IEEE Electron Device Lett. **27**, 297 (2006).

⁷A. S. Verhulst, W. G. Vandenberghe, K. Maex, and G. Groeseneken, Appl. Phys. Lett. **91**, 053102 (2007).

⁸T. Uemura and T. Baba, Solid-State Electron. **40**, 519 (1996).

⁹W. M. Reddick and G. A. Amaratunga, Appl. Phys. Lett. **67**, 494 (1995).

¹⁰J. Koga and A. Toriumi, Appl. Phys. Lett. **70**, 2138 (1997).

¹¹C. Aydin, A. Zaslavsky, S. Luryi, S. Cristoloveanu, D. Mariolle, D. Fraboulet, and S. Deleonibus, Appl. Phys. Lett. **84**, 1780 (2004).

¹²T. Nirschl, P. F. Wang, C. Weber, J. Sedlmeir, R. Heinrich, R. Kakoschke, K. Schrufer, J. Holz, C. Pacha, T. Schulz, M. Ostermayr, A. Olbrich, G. Georgakos, E. Ruderer, W. Hansch, and D. Schmitt-Landsiedel, Tech. Dig. - Int. Electron Devices Meet. **2004**, 195.

¹³K. R. Kim, H. H. Kim, K.-W. Song, J. I. Huh, J. D. Lee, and B.-G. Park, IEEE Trans. Nanotechnol. **4**, 317 (2005).

¹⁴J. Appenzeller, Y. M. Lin, J. Knoch, and P. Avouris, Phys. Rev. Lett. **93**, 196805 (2004).

¹⁵J. Appenzeller, L. Yu-Ming, J. Knoch, C. Zhihong, and P. Avouris, IEEE Trans. Electron Devices **52**, 2568 (2005).

¹⁶S. O. Koswatta, D. E. Nikonov, and M. S. Lundstrom, Tech. Dig. - Int. Electron Devices Meet. **2005**, 518.

¹⁷Y. R. Lu, S. Bangsaruntip, X. R. Wang, L. Zhang, Y. Nishi, and H. J. Dai, J. Am. Chem. Soc. **128**, 3518 (2006).

¹⁸G. Zhang, X. Wang, X. Li, Y. Lu, A. Javey, and H. Dai, Tech. Dig. - Int. Electron Devices Meet. **2006**, 431.

¹⁹J. Knoch, S. Mantl, and J. Appenzeller, Solid-State Electron. **51**, 572 (2007).

²⁰W. Y. Choi, B.-G. Park, J. D. Lee, and T.-J. K. Liu, IEEE Electron Device Lett. **28**, 743 (2007).

²¹R. Saito, G. Dresselhaus, and M. S. Dresselhaus, *Physical Property of Carbon Nanotubes* (Imperial College Press, London, 1998).

²²J. Guo, J. Appl. Phys. **98**, 063519 (2005).

²³S. O. Koswatta, S. Hasan, M. S. Lundstrom, M. P. Anantram, and D. E. Nikonov, IEEE Trans. Electron Devices **54**, 2339 (2007).

²⁴A. Javey, J. Guo, D. B. Farmer, Q. Wang, E. Yenilmez, R. G. Gordon, M. Lundstrom, and H. J. Dai, Nano Lett. **4**, 1319 (2004).

²⁵S. O. Koswatta, M. S. Lundstrom, and D. E. Nikonov, Nano Lett. **7**, 1160 (2007).

²⁶M. Pourfath, H. Kosina, and S. Selberherr, J. Phys.: Conf. Ser. **38**, 29 (2006).

²⁷S. O. Koswatta, M. S. Lundstrom, M. P. Anantram, and D. E. Nikonov, Appl. Phys. Lett. **87**, 3 (2005).

²⁸S. Datta, *Quantum Transport: Atom to Transistor* (Cambridge University Press, Cambridge, 2005).

²⁹R. Venugopal, Z. Ren, S. Datta, M. S. Lundstrom, and D. Jovanovic, J. Appl. Phys. **92**, 3730 (2002).

³⁰S. Hasan, M. A. Alam, and M. S. Lundstrom, IEEE Trans. Electron Devices **54**, 2352 (2007).

³¹E. M. Conwell, Phys. Rev. B **22**, 1761 (1980).

³²C. Rivas, R. Lake, G. Klimeck, W. R. Frensley, M. V. Fischetti, P. E. Thompson, S. L. Rommel, and P. R. Berger, Appl. Phys. Lett. **78**, 814 (2001).



Influence of phonon scattering on the performance of p - i - n band-to-band tunneling transistors

Siyuranga O. Koswatta, Mark S. Lundstrom, and Dmitri E. Nikonov

Citation: [Applied Physics Letters](#) **92**, 043125 (2008); doi: 10.1063/1.2839375

View online: <http://dx.doi.org/10.1063/1.2839375>

View Table of Contents: <http://scitation.aip.org/content/aip/journal/apl/92/4?ver=pdfcov>

Published by the [AIP Publishing](#)

Articles you may be interested in

[Optimizing transistor performance of percolating carbon nanotube networks](#)

Appl. Phys. Lett. **97**, 043111 (2010); 10.1063/1.3469930

[The effect of acoustic phonon scattering on the carrier mobility in the semiconducting zigzag single wall carbon nanotubes](#)

Appl. Phys. Lett. **96**, 183108 (2010); 10.1063/1.3427419

[The performance volatility of carbon nanotube-based devices: Impact of ambient oxygen](#)

Appl. Phys. Lett. **95**, 123118 (2009); 10.1063/1.3236779

[Deformation potential carrier-phonon scattering in semiconducting carbon nanotube transistors](#)

Appl. Phys. Lett. **90**, 062110 (2007); 10.1063/1.2437127

[Role of phonon scattering in carbon nanotube field-effect transistors](#)

Appl. Phys. Lett. **86**, 193103 (2005); 10.1063/1.1923183

A promotional banner for a webinar series. The background shows a person in a lab coat working with a piece of scientific equipment. The text 'WHAT YOU NEED TO KNOW ABOUT VACUUM' is in yellow and white. Below it, 'WEBINAR SERIES' is in white on a pink background. To the right, 'SIGN UP TODAY' is in white on a blue background with pink arrowheads. The Agilent Technologies logo is at the bottom.